Supporting Information

A Positron Emission Tomography Imaging Probe Selectively Targeting BD1 of Bromodomain and Extra-terminal Domain

Ping Bai[1], Yan Liu[1], Frederick A. Bagdasarian[1], Moses Q. Wilks[2], Hsiao-Ying Wey[1], Changning Wang[1*]

[1]Athinoula A. Martinos Center for Biomedical Imaging, Department of Radiology, Massachusetts General Hospital, Harvard Medical School, Charlestown, MA 02129, United States

[2]Gordon Center for Medical Imaging, Massachusetts General Hospital, Harvard Medical School, Charlestown, Massachusetts 02129, United States

*To whom correspondence should be addressed:

Changning Wang, PhD

Martinos Center for Biomedical Imaging at Massachusetts General Hospital, Harvard Medical School

149 13th Street, Suite 2301

Charlestown, MA 02129

617-724-3983

cwang15@mgh.harvard.edu

Table of Contents

Synthesis and Structure-activity Relationship Study of BD1-selective BET Inhibitors.

To investigate the impact of the substitutes on the phenyl group of **1a** on BD1 potency and selectivity, we synthesized an array of analogues and evaluated their binding affinities toward BRD4 BD1 and BD2. Compounds **1a-j** were prepared as shown in **Scheme 1**. Commercially available benzo[cd]indol-2(1H)-one was employed as the starting material to react with appropriate sulfonyl chlorides to obtain desired products **1a-h**. Compound **1i** was synthesized by demethylation of **1a**, and **1j** was prepared by hydrolysis of **1b**.

Scheme S1. Synthesis of compounds **1a-j**.[a]

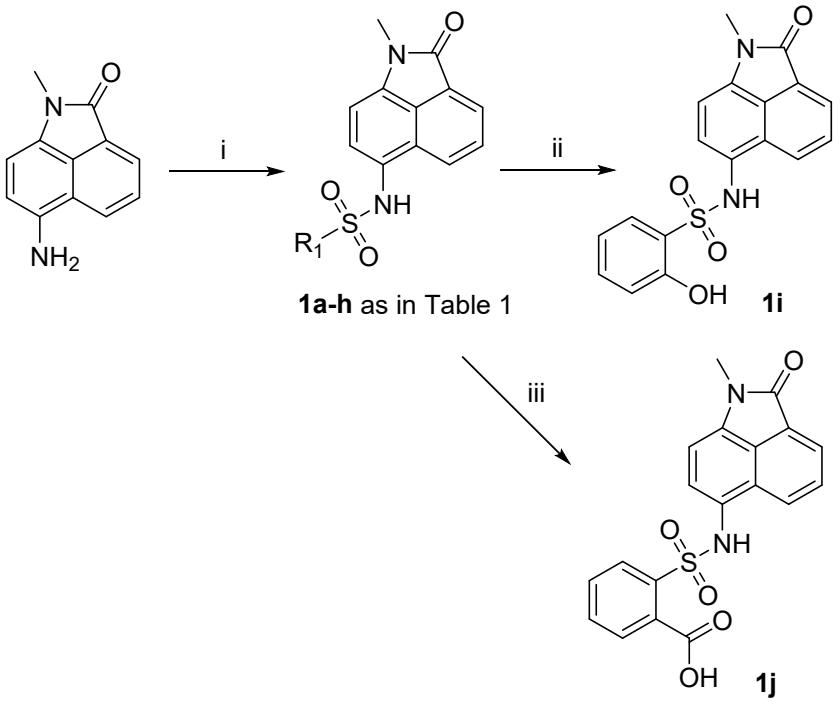

[a] Reagents and condition: (i) Appropriate sulfonyl chlorides, pyridine, dichloromethane, rt.; (ii) **1a**, BBr_3, DCM, -78°C to rt., 15 min; (iii) **1g**, $NaOH_{(aq)}$, MeOH, rt.

Table S1. Binding affinities of compounds **1a-j** toward BRD4 BD1 and BRD4 BD2.[a]

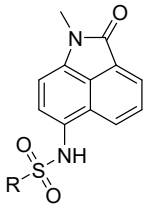

Cpd.	R	BRD4 binding affinities (BROMOScan, K_d)		
		BD1 (nM)	BD2 (nM)	Selectivity (BD2/BD1)
1a	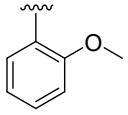	19	880	46.3
1b	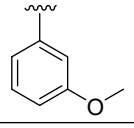	470	1900	4.0
1c	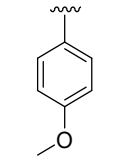	1100	6000	1.4
1d	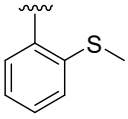	40	820	20.5
1e	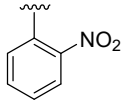	210	3100	14.7
1f	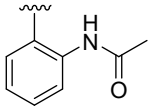	280	3500	12.5
1g	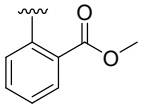	370	1600	4.3
1h	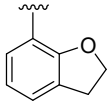	48	1600	33.3
1i	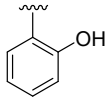	28	370	13.2
1j	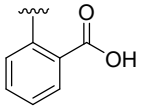	570	1200	2.1

[a]BRD binding affinities were evaluated by BROMOScan assay, K_d values represent the mean of two biological replicates.

EXPERIMENTAL SECTION

Animal procedures. The animal studies in this paper were carried out at Massachusetts General Hospital (PHS Assurance of Compliance No. A3596-01). The Subcommittee on Research Animal Care (SRAC) serves as the Institutional Animal Care and Use Committee (IACUC) for the Massachusetts General Hospital (MGH). SRAC reviewed and approved all procedures detailed in this paper.

Materials and Methods. All reagents and solvents were obtained from commercial sources, including Sigma-Aldrich (St. Louis, MO), Acros Organics. The analytical separation was conducted on an Agilent 1100 series HPLC fitted with a diode-array detector, quaternary pump, vacuum degasser, and autosampler. Analytical thin-layer chromatography (TLC) was performed on silica gel GF254. NMR spectra were collected in a JEOL NMR-ECZ500R Spectrometer at room temperature (500 MHz (^{1}H), 471 MHz (^{19}F), and 126 MHz (^{13}C)). Chemical shifts were given in δ values (ppm), using tetramethylsilane (TMS) as the internal standard. Mass spectrometry data were recorded on an Agilent 6310 ion trap mass spectrometer (ESI source) connected to an Agilent 1200 series HPLC with a quaternary pump, vacuum degasser, diode-array detector, and autosampler.

Chemistry. The purity of all compounds was determined by an analytical HPLC method and was found to be greater than 95% for all compounds.

General procedure for the synthesis of compound 1a-h. To a solution of 6-amino-1-methylbenzo[cd]indol-2(1H)-one (500 mg, 2.5 mmol) and appropriate sulfonyl chlorides (2.75 mmol) in anhydrous dichloromethane (10 mL) was added pyridine (0.5 mL). The mixture was stirred for 4-8 h at room temperature. After the complete consumption of 6-amino-1-methylbenzo[cd]indol-2(1H)-one, the reaction solution was concentrated under reduced pressure and the crude product was purified through CombiFlash chromatography (0% - 2% CH_3OH in CH_2Cl_2) to afford the desired compounds.

2-methoxy-N-(1-methyl-2-oxo-1,2-dihydrobenzo[cd]indol-6-yl)benzenesulfonamide (**1a**). Yellow solid; yield: 61.5%. ^{1}H NMR (500 MHz, $CDCl_3$) δ 8.20 (d, *J* = 8.3 Hz, 1H), 8.01 (d, *J* = 7.0 Hz, 1H), 7.73 – 7.65 (m, 2H), 7.49 (ddd, *J* = 8.7, 7.4, 1.7 Hz, 1H), 7.29 (s, 1H), 7.10 (d, *J* = 7.5 Hz, 1H), 7.03 (d, *J* = 8.4 Hz, 1H), 6.96 – 6.89 (m, 1H), 6.65 (d, *J* = 7.6 Hz, 1H), 4.08 (s, 3H), 3.34 (s, 3H). ^{13}C NMR (126 MHz, $CDCl_3$) δ 168.2, 158.1, 139.0,

135.1, 130.9, 129.0, 127.2, 127.0, 126.8, 125.5, 124.9, 124.2, 120.9, 112.2, 104.5, 77.3, 77.1, 76.8, 56.6, 26.3. HRMS calculated for $C_{19}H_{16}N_2O_4S$: 368.0831; Found $[M + H]^+$: 369.0928.

3-methoxy-N-(1-methyl-2-oxo-1,2-dihydrobenzo[cd]indol-6-yl)benzenesulfonamide (**1b**). Yellow solid; yield: 55.6%. ^{1}H NMR (500 MHz, $CDCl_3$) ^{1}H NMR (500 MHz, Chloroform-*d*) δ 8.00 (t, *J* = 5.7 Hz, 1H), 7.92 (d, *J* = 8.4 Hz, 1H), 7.61 (dd, *J* = 8.4, 6.8 Hz, 1H), 7.28 – 7.24 (m, 2H), 7.22 – 7.17 (m, 2H), 7.07 – 6.99 (m, 2H), 6.75 (t, *J* = 6.4 Hz, 1H), 3.68 (s, 3H), 3.42 (s, 3H). ^{13}C NMR (126 MHz, $CDCl_3$) δ 168.3, 1157.2, 129.6, 129.1 (2C), 127.1, 126.7 (2C), 126.3, 124.8, 114.2, 104.7, 77.3, 77.13, 76.8, 55.6, 26.4. HRMS calculated for $C_{19}H_{16}N_2O_4S$: 368.0831; Found $[M + H]^+$: 369.0825.

4-methoxy-N-(1-methyl-2-oxo-1,2-dihydrobenzo[cd]indol-6-yl)benzenesulfonamide (**1c**). Yellow solid; yield: 57.1%. ^{1}H NMR (500 MHz, $CDCl_3$) δ 8.00 (dd, *J* = 7.0, 2.1 Hz, 1H), 7.96 (dd, *J* = 8.3, 2.4 Hz, 1H), 7.65 – 7.61 (m, 2H), 7.17 (dd, *J* = 7.6, 2.2 Hz, 1H), 6.99 (s, 1H), 6.84 – 6.79 (m, 2H), 6.73 (dd, *J* = 7.5, 2.3 Hz, 1H), 3.78 (s, 3H), 3.39 (s, 3H). ^{13}C NMR (126 MHz, $CDCl_3$) δ 139.0, 135.1, 130.9, 129.0, 127.2, 127.0, 126.8, 125.5, 124.9, 124.2, 120.9, 112.2, 104.5, 77.3, 77.1, 76.8, 56.6, 26.3. HRMS calculated for $C_{19}H_{16}N_2O_4S$: 368.0831; Found $[M + H]^+$: 369.0830.

N-(1-methyl-2-oxo-1,2-dihydrobenzo[cd]indol-6-yl)-2-(methylthio)benzenesulfonamide (**1d**). Yellow solid; yield: 57.5%. ^{1}H NMR (500 MHz, $CDCl_3$) δ 8.18 (d, *J* = 8.3 Hz, 1H), 8.01 (d, *J* = 6.9 Hz, 1H), 7.70 – 7.65 (m, 2H), 7.60 (s, 1H), 7.48 – 7.40 (m, 2H), 7.10 – 7.03 (m, 2H), 6.65 (d, *J* = 7.5 Hz, 1H), 3.35 (s, 3H), 2.67 (s, 3H). ^{13}C NMR (126 MHz, $CDCl_3$) δ 168.2, 133.2, 130.91, 129.1, 127.2 (2C), 126.56 (2C), 125.5 (2C), 125.1, 124.9, 104.5, 77.3, 77.13, 76.8, 26.4, 16.7. HRMS calculated for $C_{19}H_{16}N_2O_3S_2$: 384.0602; Found $[M + H]^+$: 385.0589.

N-(1-methyl-2-oxo-1,2-dihydrobenzo[cd]indol-6-yl)-2-nitrobenzenesulfonamide (**1e**). Yellow solid; yield: 61.5%. ^{1}H NMR (500 MHz, $CDCl_3$) ^{1}H NMR (500 MHz, Chloroform-*d*) δ 8.11 (dd, *J* = 8.3, 2.5 Hz, 1H), 8.03 (d, *J* = 6.9 Hz, 1H), 7.90 (dd, *J* = 8.0, 1.2 Hz, 1H), 7.70 – 7.66 (m, 1H), 7.66 – 7.63 (m, 2H), 7.52 (s, 1H), 7.48 (td, *J* = 7.7, 1.3 Hz, 1H), 7.28 (d, *J* = 7.5 Hz, 1H), 6.76 (d, *J* = 7.5 Hz, 1H), 3.40 (s, 3H). ^{13}C NMR (126 MHz, DMSO-d_6) δ 167.2, 135.1, 132.8, 130.8, 129.6, 128.1, 127.7, 126.6 (2C), 125.2 (2C), 106.1 (2C), 40.0 (2C), 26.74. HRMS calculated for $C_{19}H_{16}N_2O_4S$: 383.057; Found $[M + H]^+$: 384.0601.

N-(2-(N-(1-methyl-2-oxo-1,2-dihydrobenzo[cd]indol-6-yl)sulfamoyl)phenyl)acetamide (**1f**). Yellow solid; yield: 47.3%. ^{1}H NMR (500 MHz, $CDCl_3$) δ 8.12 (d, *J* = 6.9 Hz, 1H), 8.08 (d, *J* = 8.2 Hz, 1H), 7.81 (dd, *J* = 8.3, 7.0 Hz, 1H), 7.72 (dd, *J* = 8.1, 1.5 Hz, 1H), 7.52 (d, *J* = 7.5 Hz, 1H), 7.37 – 7.32 (m, 1H), 6.93 (d, *J* = 7.5 Hz, 1H), 6.76 – 6.71 (m, 2H), 3.46 (s, 3H), 1.86 (s, 3H). ^{13}C NMR (126 MHz, $CDCl_3$) δ 159.2, 139.0, 135.1, 130.9 (2C),

129.0 (2C), 127.2, 127.0, 126.8, 125.5, 124.9, 124.2, 120.9, 112.2, 104.5, 77.3, 77.1, 76.8, 56.6, 26.3. HRMS calculated for $C_{20}H_{17}N_3O_4S$: 395.0940; Found $[M + H]^+$: 396.0886.

methyl 2-(N-(1-methyl-2-oxo-1,2-dihydrobenzo[cd]indol-6-yl)sulfamoyl)benzoate (**1g**). Yellow solid; yield: 52.8%. ^{1}H NMR (500 MHz, $CDCl_3$) δ 8.26 (s, 1H), 8.14 (dd, *J* = 8.2, 1.9 Hz, 1H), 7.99 (dd, *J* = 7.1, 1.7 Hz, 1H), 7.84 (dt, *J* = 7.7, 1.7 Hz, 1H), 7.65 – 7.60 (m, 2H), 7.57 (tq, *J* = 7.6, 1.4 Hz, 1H), 7.38 (ddt, *J* = 9.1, 7.7, 1.3 Hz, 1H), 7.21 (dd, *J* = 7.8, 1.6 Hz, 1H), 6.71 (dd, *J* = 7.5, 1.6 Hz, 1H), 4.11 (s, 3H), 3.39 (s, 3H). ^{13}C NMR (126 MHz, $CDCl_3$) δ 157.2, 139.0, 135.1, 130.9, 129.0 (2C), 127.2, 127.0, 126.8, 125.5 (2C), 124.9, 124.2, 120.9, 112.2, 104.5, 77.3, 77.1, 76.8, 56.6, 26.3. HRMS calculated for $C_{20}H_{16}N_2O_5S$: 396.0780; Found $[M + H]^+$: 397.0753.

N-(1-methyl-2-oxo-1,2-dihydrobenzo[cd]indol-6-yl)-2,3-dihydrobenzofuran-7-sulfonamide (**1h**). Yellow solid; yield: 50.2%. ^{1}H NMR (500 MHz, $CDCl_3$) δ 8.16 (d, *J* = 8.3 Hz, 1H), 8.02 (d, *J* = 7.1 Hz, 1H), 7.69 (dd, *J* = 8.2, 7.0 Hz, 1H), 7.39 (d, *J* = 7.9 Hz, 1H), 7.30 (d, *J* = 7.3 Hz, 1H), 7.22 (d, *J* = 7.6 Hz, 1H), 7.14 (s, 1H), 6.78 (t, *J* = 7.6 Hz, 1H), 6.70 (d, *J* = 7.6 Hz, 1H), 4.77 (t, *J* = 8.8 Hz, 2H), 3.35 (s, 3H), 3.24 (t, *J* = 8.8 Hz, 2H). ^{13}C NMR (126 MHz, $CDCl_3$) δ 168.2, 156.1, 130.1 (2C), 129.02, 128.0, 126.9 (2C), 124.8, 124.1, 120.7 (2C), 104.7, 77.3, 77.1, 76.8, 73.2, 29.8, 29.1, 26.4. HRMS calculated for $C_{20}H_{16}N_2O_4S$: 380.0831; Found $[M + H]^+$: 381.0826.

2-hydroxy-N-(1-methyl-2-oxo-1,2-dihydrobenzo[cd]indol-6-yl)benzenesulfonamide (**1i**). To a solution of **1a** (100 mg, 0.27 mmol) in anhydrous dichloromethane (10 mL) was added BBr_3 (1.36 mL, 1.0 mol/L in dichloromethane) drop wisely at –78 °C under N_2. The resulting mixture was stirred for 15 min at room temperature. Then the crude product was purified using CombiFlash chromatography (0% - 2% CH_3OH in CH_2Cl_2) to afford **1i**. Yellow solid; yield: 61.5%. ^{1}H NMR (500 MHz, $CDCl_3$) δ 8.16 (d, *J* = 8.3 Hz, 1H), 8.02 (d, *J* = 7.1 Hz, 1H), 7.69 (dd, *J* = 8.3, 6.9 Hz, 1H), 7.39 (dd, *J* = 8.0, 1.2 Hz, 1H), 7.30 (dd, *J* = 7.4, 1.3 Hz, 1H), 7.22 (d, *J* = 7.5 Hz, 1H), 7.16 (s, 1H), 6.78 (t, *J* = 7.7 Hz, 1H), 6.69 (d, *J* = 7.6 Hz, 1H), 3.35 (s, 3H). ^{13}C NMR (126 MHz, $CDCl_3$) δ 169.2, 138.6, 134.5, 133.4, 130.7 (2C), 129.8, 129.3 (2C), 128.4, 127.6, 126.5, 126.3, 125.0, 124.8, 106.1, 40.04, 26.7. HRMS calculated for $C_{18}H_{14}N_2O_4S$: 354.0674; Found $[M + H]^+$: 355.0628.

2-(N-(1-methyl-2-oxo-1,2-dihydrobenzo[cd]indol-6-yl)sulfamoyl)benzoic acid (**1j**). To a solution of **1g** (100 mg, 0.26 mmol) in methanol (10 mL) was added 2M NaOH (2 mL) at room temperature. The resulting mixture was stirred for 1 h min at room temperature. After the complete consumption of **1g**, the reaction was added 5 mL H_2O and methanol was removed under reduced pressure. Then the solution was acidified with 3N HCl and extraction with EtOAc. The organic layer was concentrated, and the crude product was purified using CombiFlash chromatography (0% - 2% CH_3OH in CH_2Cl_2) to afford **1j**. Yellow solid; yield: 50.7%. ^{1}H NMR (126 MHz,

DMSO-d_6) δ 9.86 (s, 1H), 8.13 (dd, J = 8.3, 2.9 Hz, 1H), 7.94 (t, J = 5.3 Hz, 1H), 7.65 (ddt, J = 6.1, 4.7, 2.1 Hz, 2H), 7.58 (tt, J = 7.6, 2.0 Hz, 1H), 7.50 (dt, J = 8.1, 2.0 Hz, 1H), 7.43 – 7.38 (m, 1H), 7.19 (dd, J = 8.0, 2.9 Hz, 1H), 7.04 – 6.99 (m, 1H), 3.34 (s, 3H). ^{13}C NMR (126 MHz, DMSO-d_6) δ 168.9, 139.2, 138.1, 132.7, 131.6, 130.7, 130.5 (2C), 130.2, 129.1 (2C), 127.4, 127.0, 126.7 (2C), 126.4, 125.9, 125.5, 124.8, 104.6, 77.4, 77.1, 76.8, 53.8, 26.4. HRMS calculated for $C_{19}H_{14}N_2O_5S$: 382.0623; Found $[M + H]^+$: 383.0645.

Radiochemistry [^{11}C]CO_2 (1.2 Ci) was obtained *via* the ^{14}N (p, α) ^{11}C reaction on nitrogen with 2.5% oxygen, with 11 MeV protons (Siemens Eclipse cyclotron, Siemens Healthcare GmbH, Erlangen, Germany), and trapped on molecular sieves in a TRACERlab FX-MeI synthesizer (General Electric, GE Healthcare, Boston, MA, USA). [^{11}C]CH_4 was obtained by the reduction of [^{11}C]CO_2 in the presence of Ni/hydrogen at 350 °C and recirculated through an oven containing I_2 to produce [^{11}C]CH_3I *via* a radical reaction. Then [^{11}C]CH_3I was bubbled through a solution of **1i** (1 mg) and 1M NaOH (10 μL) in anhydrous DMF (0.3 mL). The mixture was stirred at 100°C for 3 min. Then to the mixture was added 1.2 mL water followed by injecting into a reverse phase semi-preparative HPLC (Phenomenex Luna 5u C18(2), eluting with a mobile phase of 64% H_2O + 0.1% TFA/36% CH_3CN, at the flow rate of 5.0 mL/min) for purification. [^{11}C]**1a** was prepared in an average of 30-40 minutes. The average radiochemical yield was 25−30% (nondecay corrected to trapped [^{11}C]CH_3I) with the purity over 95% and average molar radioactivity = 302 GBq/μmol, n = 4. The validation of [^{11}C]**1a** was conducted by co-injecting unlabeled **1a** into analysis HPLC (**Figure S2**).

BRD4 Binding Assays.[1] The binding affinities of target compounds toward all 8 bromodomains were carried out using the BROMOscan™ Platform. (DiscoverX Corp, Fremont, CA, https://www.discoverx.com). K_d values were calculated with a standard dose-response curve.

Rodent PET/CT Acquisition and Post Processing. The general procedure for rodent PET/CT imaging studies was described previously.[2, 3] Briefly, 6-month old male C57BL/6 mice were anesthetized with 2% isoflurane (Patterson Vet Supply, Inc., Greeley, CO, USA) and arranged in a Triumph Trimodality PET/CT scanner (Gamma Medica, Northridge, CA, USA). [^{11}C]**1a** (3.7-7.4 Mbq per animal) was injected via a lateral tail vein catheter at the start of PET acquisition. For the blocking studies, mice were pretreated unlabeled **1a** or CW22 5 min before the radiotracer injection. Dynamic PET acquisition lasted for 60 minutes, followed by 10-minute computed tomography (CT) for anatomic co-registration. PET data were reconstructed using a 3D-MLEM method resulting

in full width at a half-maximum resolution of 1 mm. These files were imported and analyzed using PMOD (PMOD 4.01, PMOD Technologies Ltd., Zurich, Switzerland).

Rodent PET/CT Image Analysis. Dynamic PET data were collected, and the corresponding images were reconstructed by 3D-MLEM method resulting in full width at a half-maximum resolution of 1 mm. Volumes of interest (VOIs) were generated manually in the form of spheres under the guidance of high-resolution CT structural images. Time-activity curves (TACs) were exported as decay-corrected activity per unit volume. The TACs were expressed as percent injected dose per unit volume (%ID/cc) for analysis.

NHP PET/MR acquisition and post processing. A male rhesus macaque (weight = 8.9 kg) was deprived of food for 12 hours prior to the simultaneous PET/MR scanning. Anesthesia was induced with intramuscular xylazine (0.5–2.0 mg/kg) and ketamine (10 mg/kg). After endotracheal intubation, V-line and A-line was inserted and anesthetic state was maintained using isoflurane. The macaque was antecubital catheterized for radiotracer injection and a radial arterial line was placed for metabolite analysis. PET/MR images of the brain were acquired on a 3T Siemens TIM-Trio scanner with a BrainPET insert (Siemens, Munich, Germany), using an in-house built 8-channel head coil. Dynamic PET image acquisition was initiated followed by administration of [^{11}C]**1a** (Dose: 5.63 mCi). A MEMPRAGE MRI sequence was acquired 30 minutes after the start of the scan to enable anatomic co-registration. Dynamic data from the PET scan was recorded in list mode and corrected for attenuation prior to reconstruction. PET data was reconstructed using a 3D-OSEM method and binned into progressively longer time frames. Reconstructed images were converted into standard uptake values (SUV) by ratio of the PET recorded radioactivity and injected dose multiplied by the weight of the NHP.

NHP PET/MR Image Analysis. PET data were motion-corrected followed by registration to the INIA19 Template and NeuroMaps Atlas for brain imaging analysis. Image registration was carried out on high-resolution MPRAGE T1 image using a twelve degree-of-freedom linear algorithm and a nonlinear algorithm to the atlas brain. This transformation was subsequently applied to the simultaneously collected dynamic PET data. Volumes of interest (VOIs) were segmented according to the brain atlas. VOIs used to derive TAC plots were the whole brain, cerebellum, nucleus accumbens, amygdala, putamen, thalamus, hypothalamus and hippocampus. Representative SUV images were generated by averaging the dynamic PET data from 0-20 minutes following tracer injection and overlaying on the INIA19 brain template. Kinetic modeling was performed in PMOD (PMOD3.9; PMOD Technologies). The VOIs were exported from the brain regions referenced previously for

kinetic analysis. Estimations of regional V_T (mL/cm^3) were performed by 1TCM, 2TCM, and Logan Plot modeling with metabolite-corrected plasma TAC (see below). Goodness of fit was assessed for 1TCM and 2TCM via the Akaike Information Criterion (AIC) and Model Selection Criterion (MSC). Lower AIC and higher MSC values were indicative of a better fit.

Plasma and Metabolite HPLC Analysis. Arterial blood samples were collected while the macaque underwent PET imaging. Metabolite extraction and High-Performance Liquid Chromatography (HPLC) were based on previously reported methods from our institution to generate radioHPLC chromatograms for each blood sample. In brief, blood samples were centrifuged to isolate plasma. Protein precipitation was attained via the addition and mixing of plasma (1mL) to acetonitrile (1mL). This was then centrifuged for 1 minute to obtain protein-free plasma. The protein-free supernatant (1mL) was diluted in deionized water (4mL) and underwent HPLC to distinguish radiometabolites from the parent radiotracer. HPLC setup included a column-switching valve for sample concentration (online solid-phase extraction; Agilent Bond Elut Online SPE, PLRP-S, 4.6 x 12.5 mm) and subsequent separation (Agilent Eclipse Plus C18, 4.6 x 100 mm. 3.5 μm). Radiometabolite HPLC was conducted as follows: Plasma samples were placed onto the SPE concentrator column, 1%ACN and 99%H_2O at 2mL/min. After 3 min, the sample was flowed from the SPE column to the separation column under gradient conditions (Mobile Phase A: water + 0.1% formic acid; Mobile Phase B: acetonitrile + 0.1% formic acid; separation method = 95/5 - 50/50 A/B from 3 – 8 min linear gradient; 50/50 – 5/95 A/B from 8-10 min linear gradient; 5/95 A/B from 10- 11min isocratic; flow rate 2 mL/min). Analytes were then monitoring for ~10 min after sample injection via dual opposing bismuth germanium oxide detectors for coincidence detection (Eckert and Ziegler). Once generated, chromatograms were corrected for radioactive decay and subsequently integrated to quantify area under the curve for each respective metabolite and comparison to the original parent tracer. Each plasma sample's parent fraction was fit and then applied to the plasma input curve, allowing derivation of the radiometabolite-corrected plasma input function used for tissue compartment modeling discussed previously.

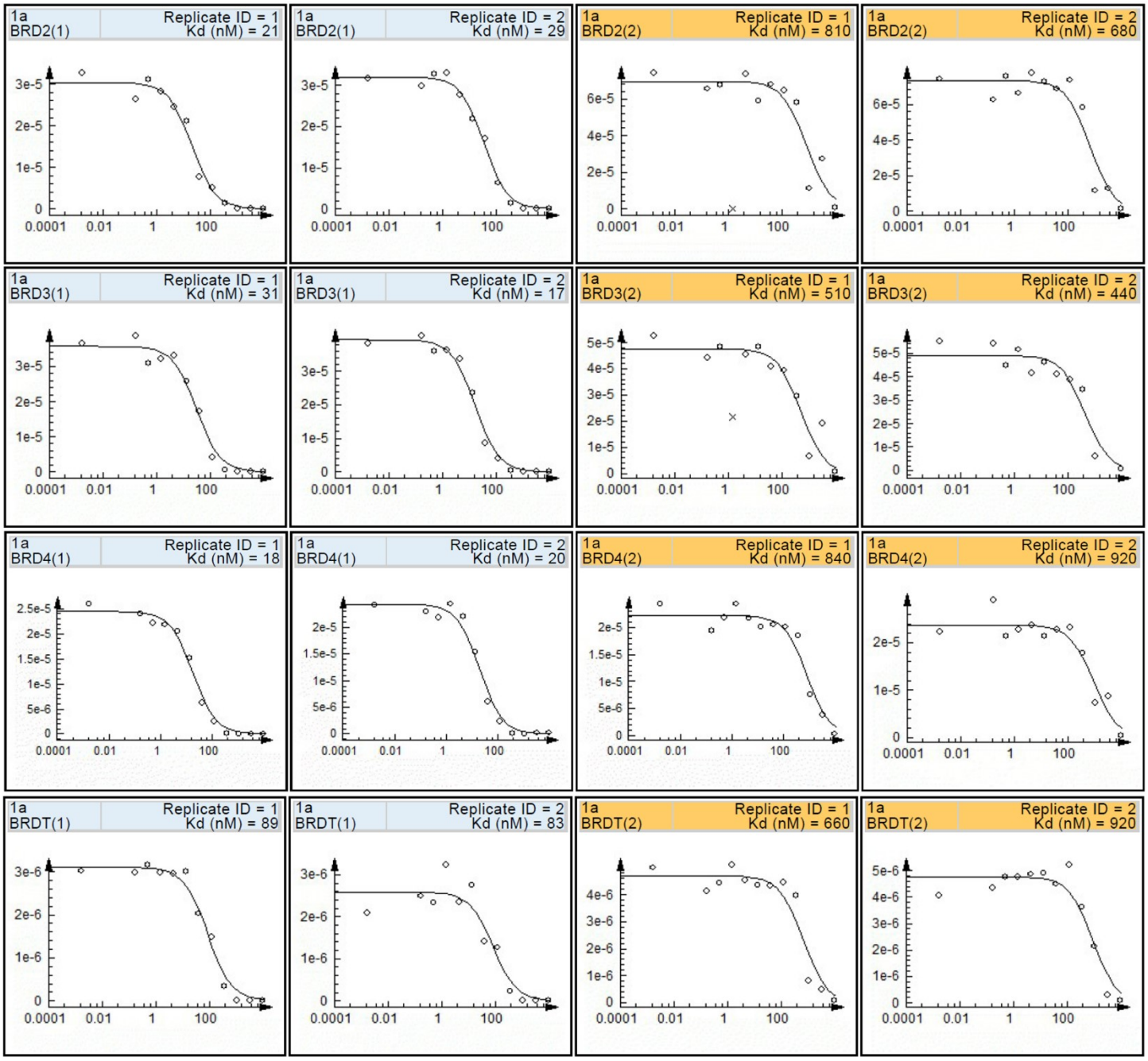

Figure S1. The K_d curve images of **1a** toward 8 BET bromodomains.

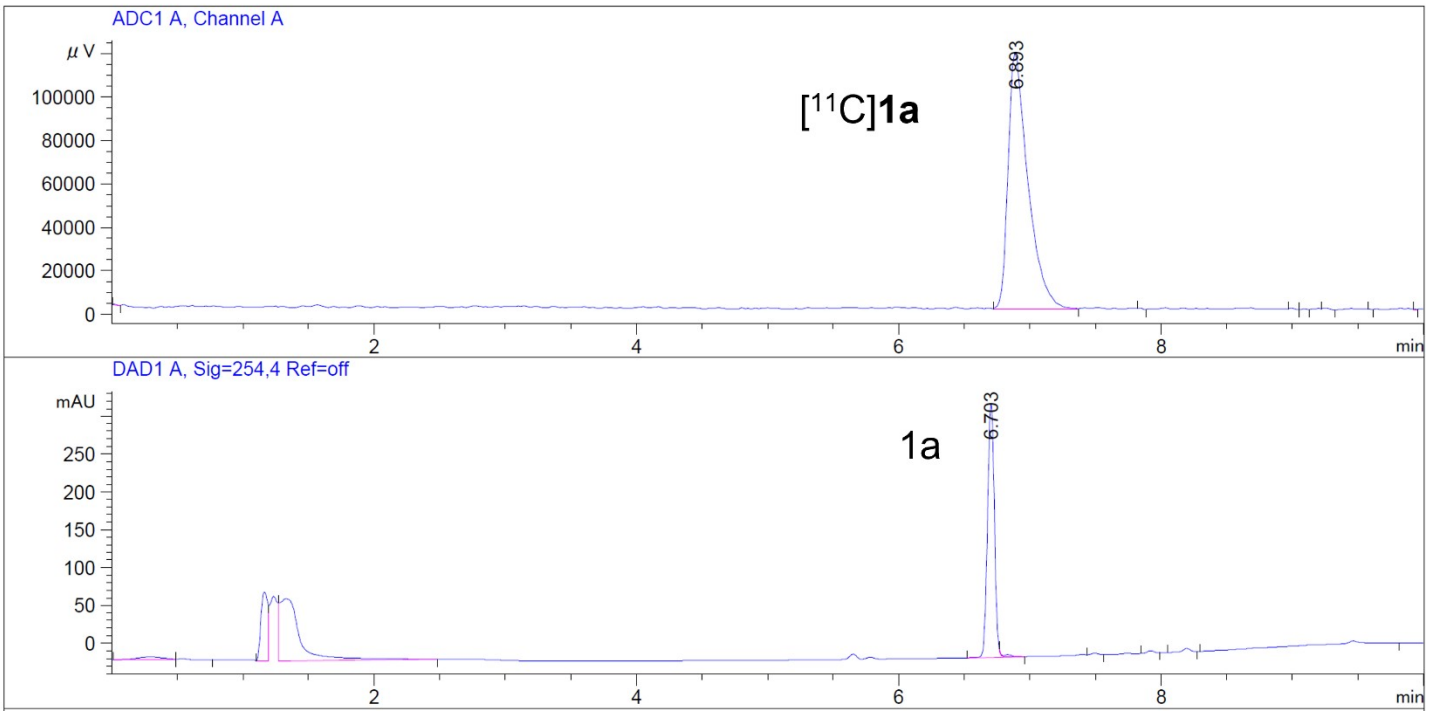

Figure S2. The HPLC chromatogram of [^{11}C]**1a**. Analytic HPLC condition: Agilent Eclipse plus C18, 3.5 μm, 4.6×100 mm, flow rate = 1.0 mL/min, mobile phase = 0.1% formic acid in water / 0.1% formic acid in acetonitrile, gradient method.

^{1}H NMR and ^{13}C NMR spectra for the synthesized compounds

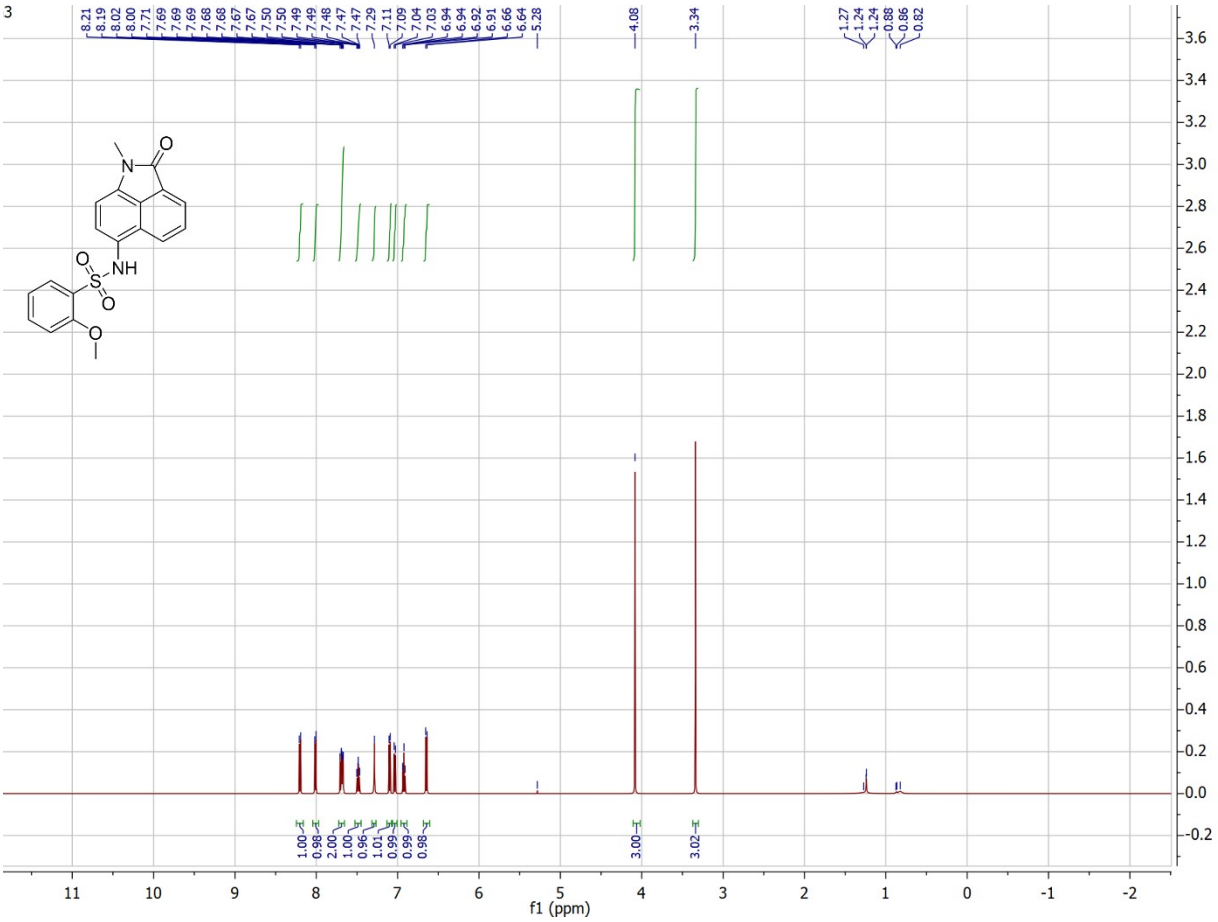

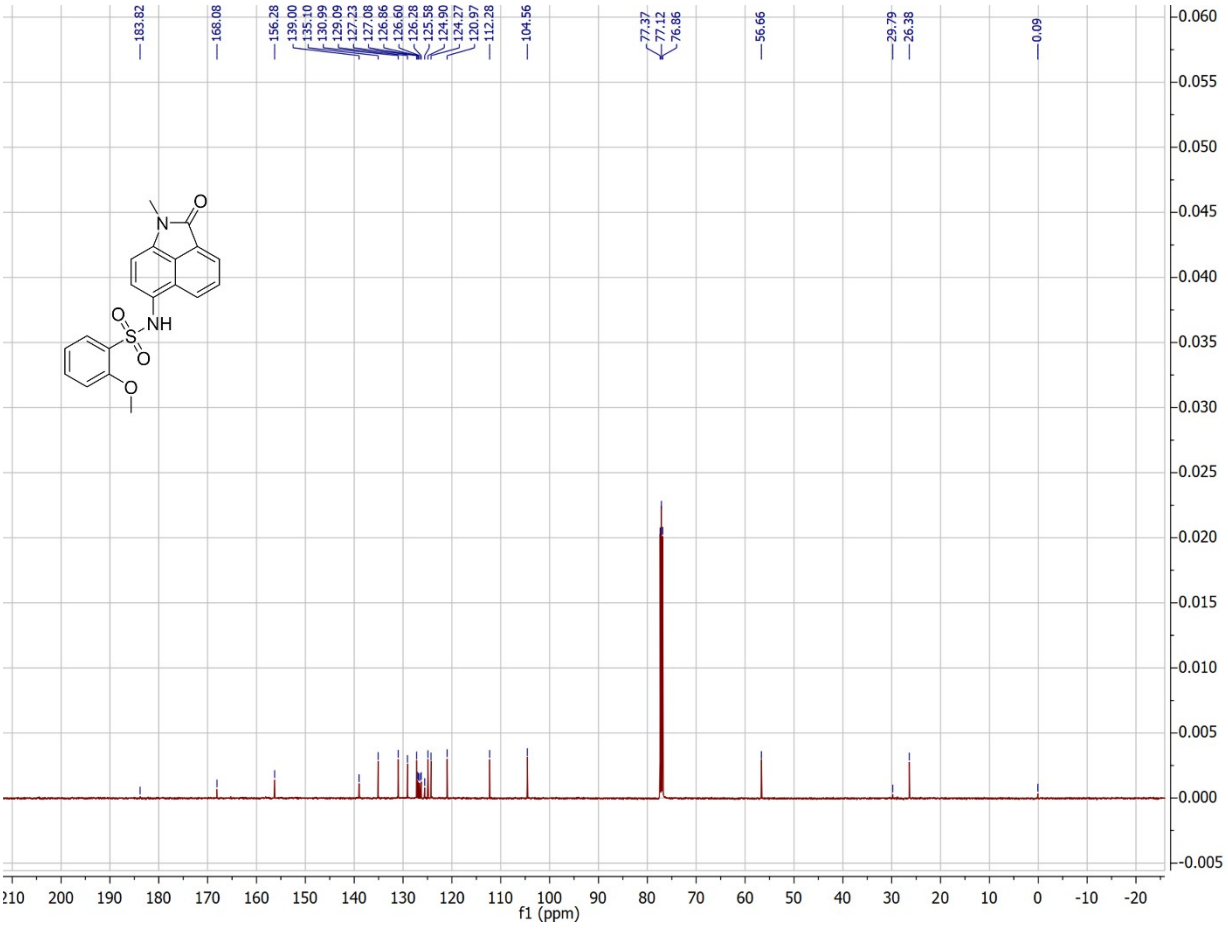
183.82
168.08
156.28
139.00
135.10
130.99
129.09
127.23
127.08
126.86
126.60
126.28
125.58
124.90
124.27
120.97
112.28
104.56
77.37
77.12
76.86
56.66
29.79
26.38
0.09
f1 (ppm)

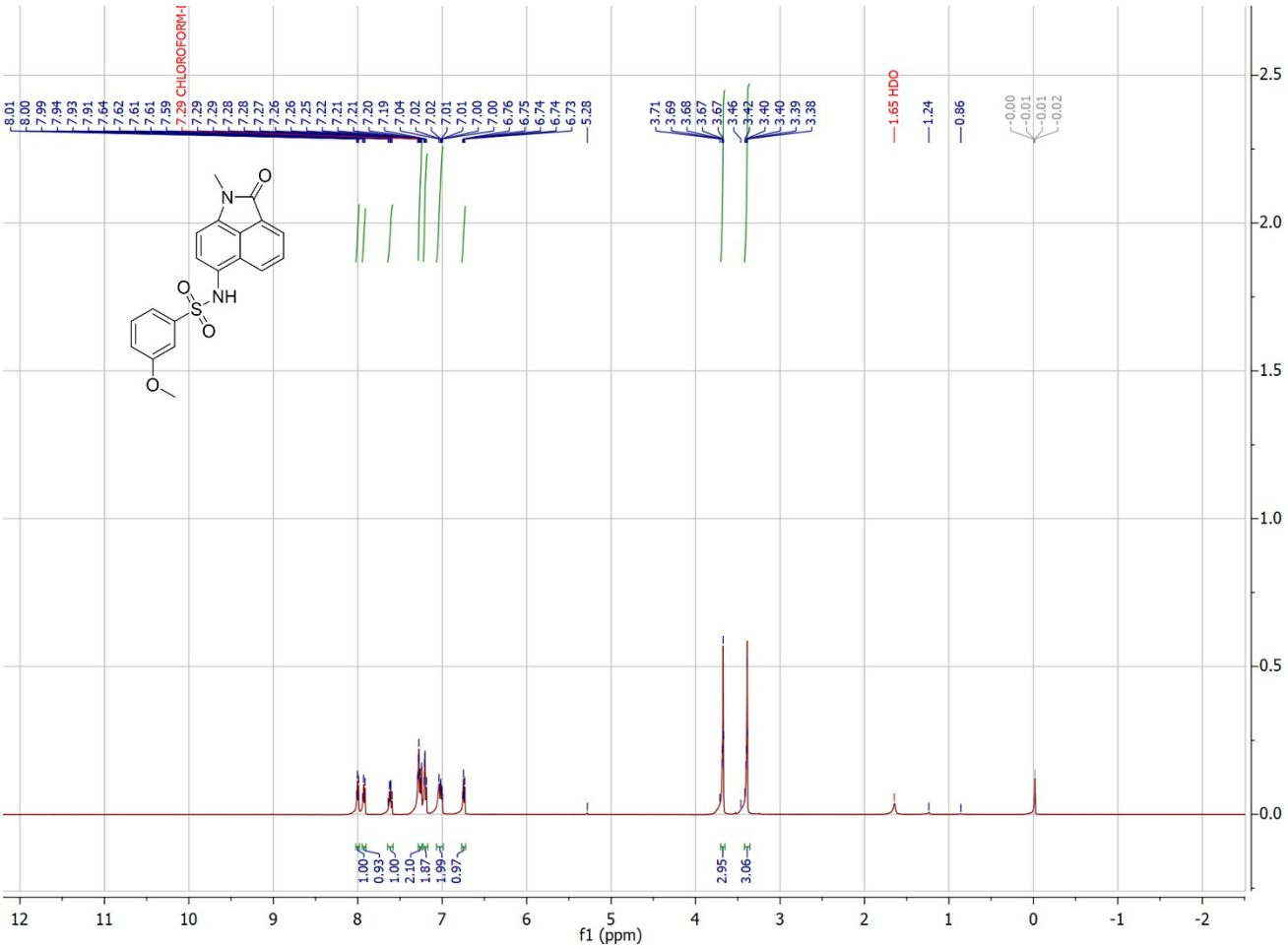
8.01
8.00
7.99
7.94
7.93
7.91
7.64
7.62
7.61
7.61
7.59
7.29 CHLOROFORM-I
7.29
7.29
7.28
7.28
7.27
7.26
7.26
7.25
7.22
7.21
7.21
7.20
7.19
7.04
7.02
7.02
7.01
7.01
7.00
7.00
6.76
6.75
6.74
6.74
6.73
5.28
3.71
3.69
3.68
3.67
3.67
3.46
3.42
3.40
3.40
3.39
3.38
1.65 HDO
1.24
0.86
0.00
0.01
0.01
0.02
1.00
0.93
1.00
2.10
1.87
1.99
0.97
2.95
3.06
f1 (ppm)

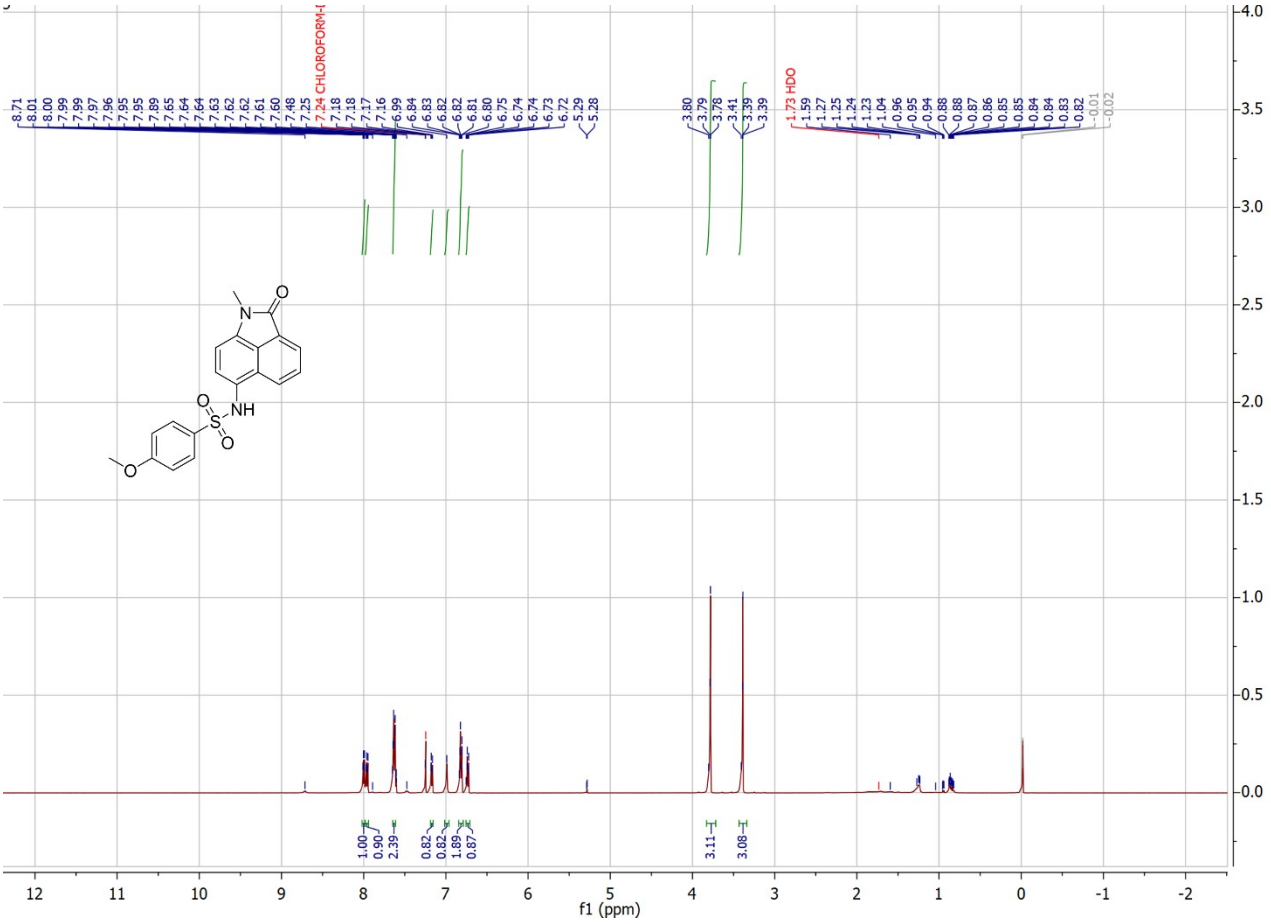
8.71
8.01
8.00
7.99
7.99
7.97
7.96
7.95
7.95
7.89
7.65
7.64
7.64
7.63
7.62
7.62
7.61
7.60
7.48
7.25
7.24 CHLOROFORM-D
7.18
7.18
7.17
7.16
6.99
6.84
6.83
6.82
6.82
6.81
6.80
6.75
6.74
6.74
6.73
6.72
5.29
5.28
3.80
3.79
3.78
3.41
3.39
3.39
1.73 HDO
1.59
1.27
1.25
1.24
1.23
1.04
0.96
0.95
0.94
0.88
0.88
0.87
0.86
0.85
0.85
0.84
0.84
0.83
0.82
-0.01
-0.02
O
N
O
NH
S
O
O
1.00
0.90
2.39
0.82
0.82
1.89
0.87
3.11
3.08
f1 (ppm)

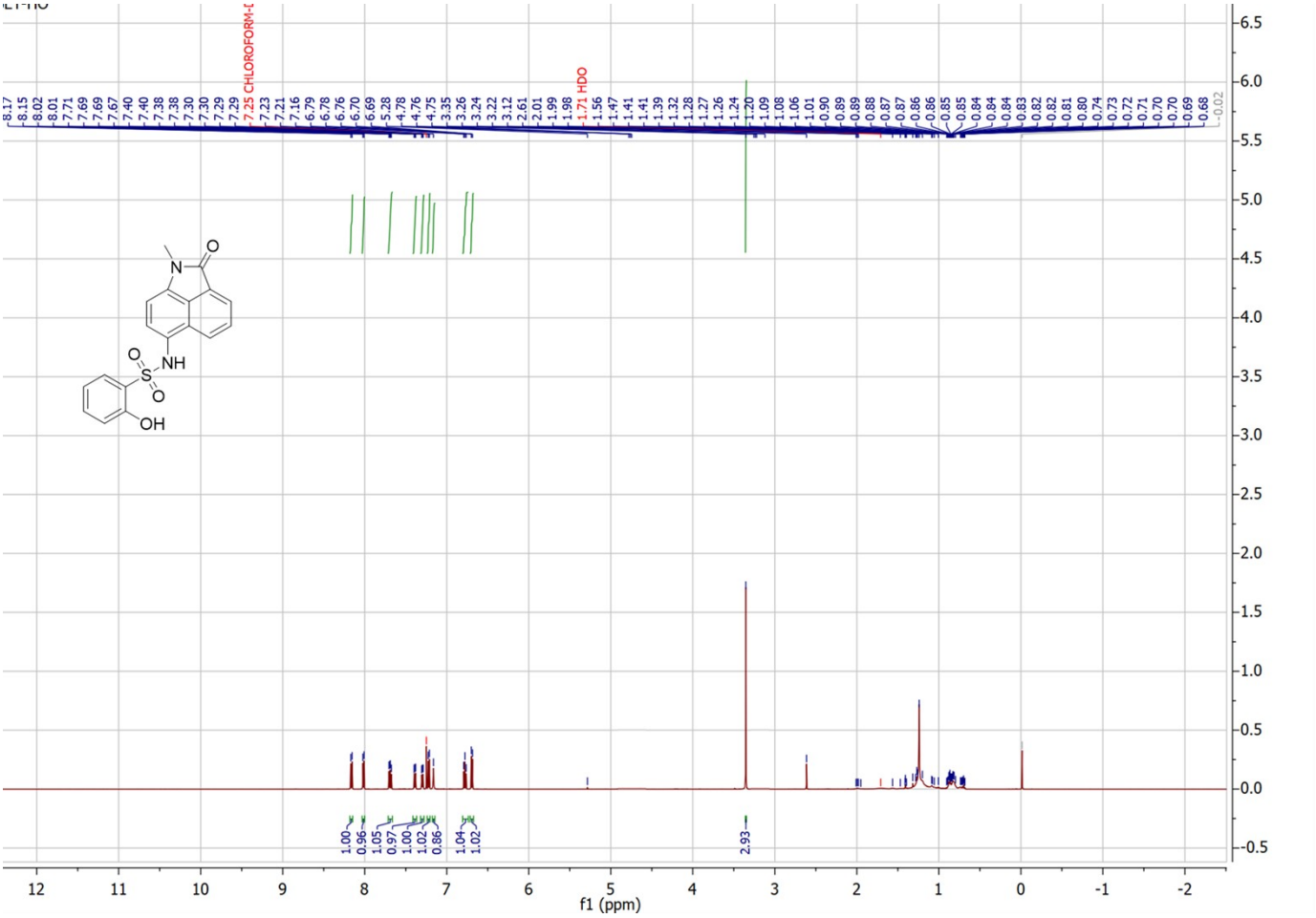
CHLOROFORM-d
HDO
f1 (ppm)

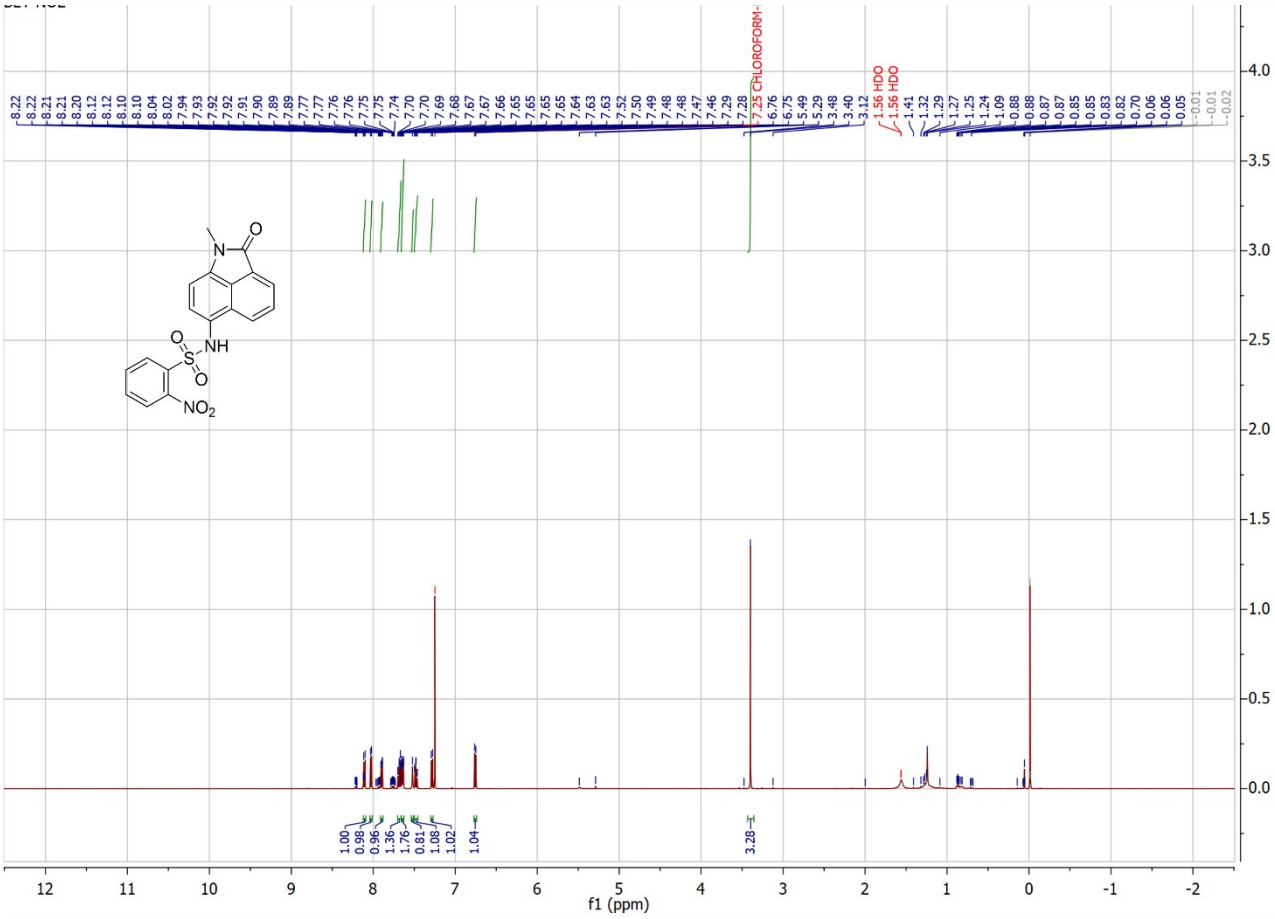
CHLOROFORM-
1.56 HDO
1.56 HDO
f1 (ppm)

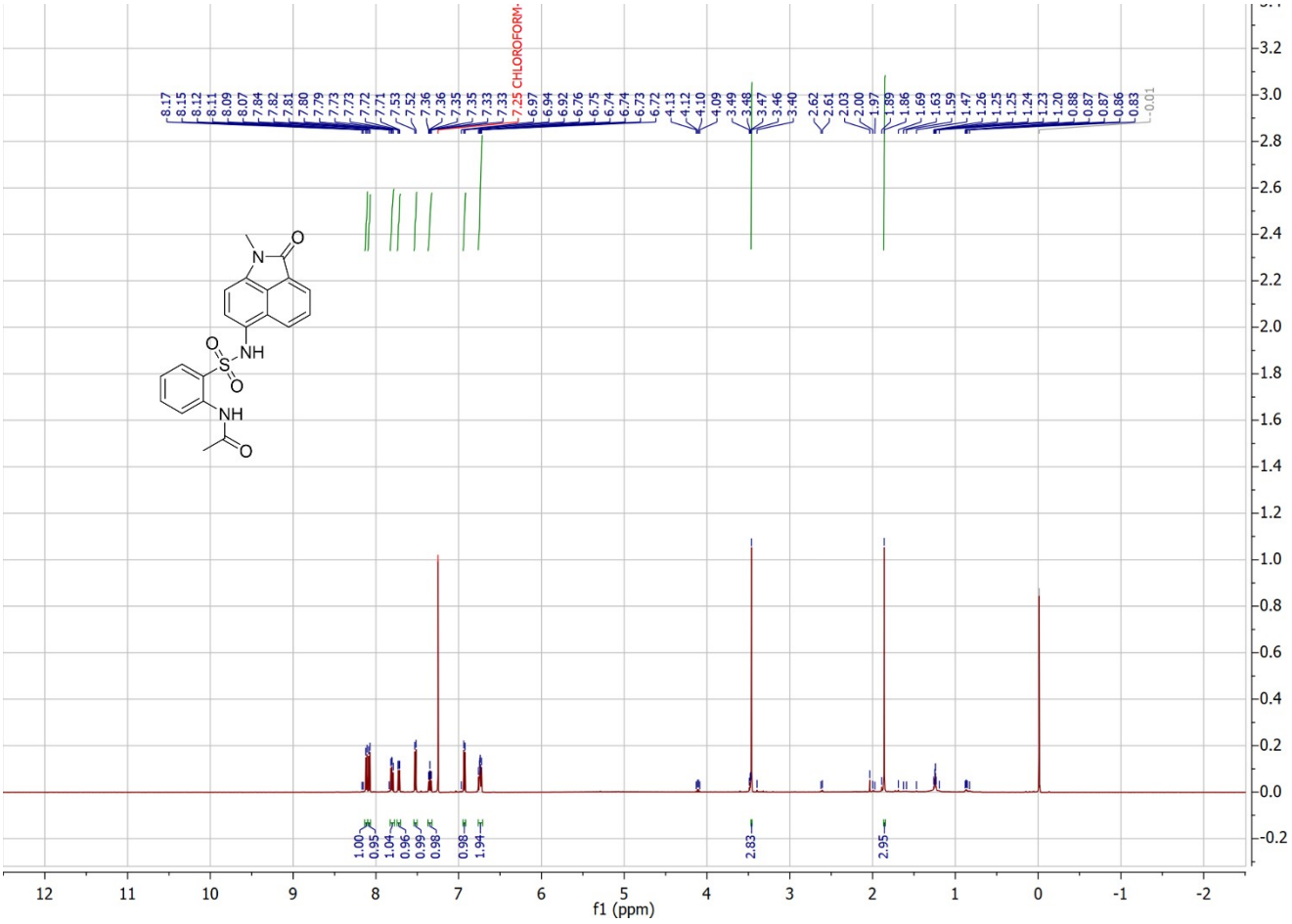
CHLOROFORM-
f1 (ppm)

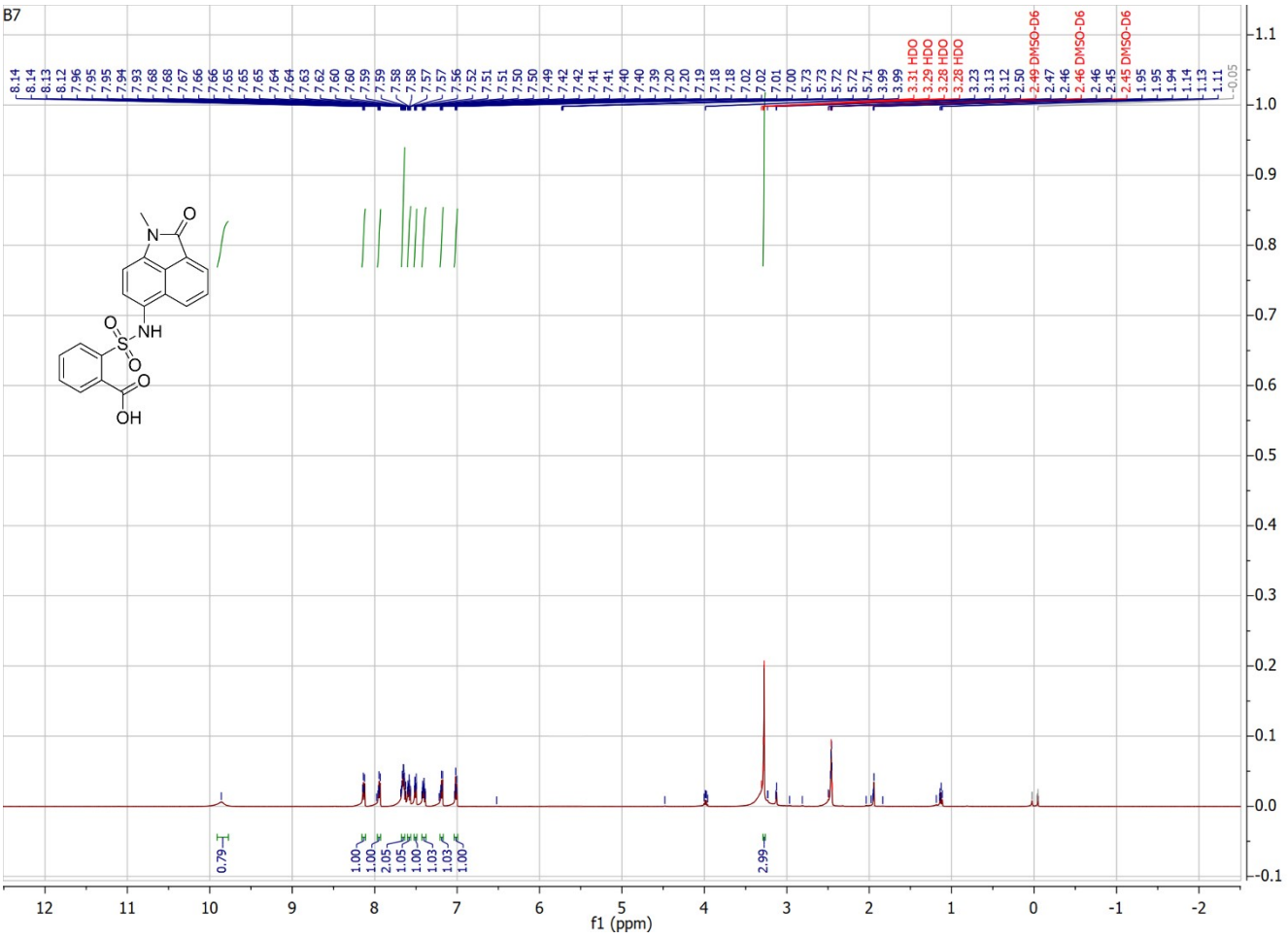
B7
f1 (ppm)

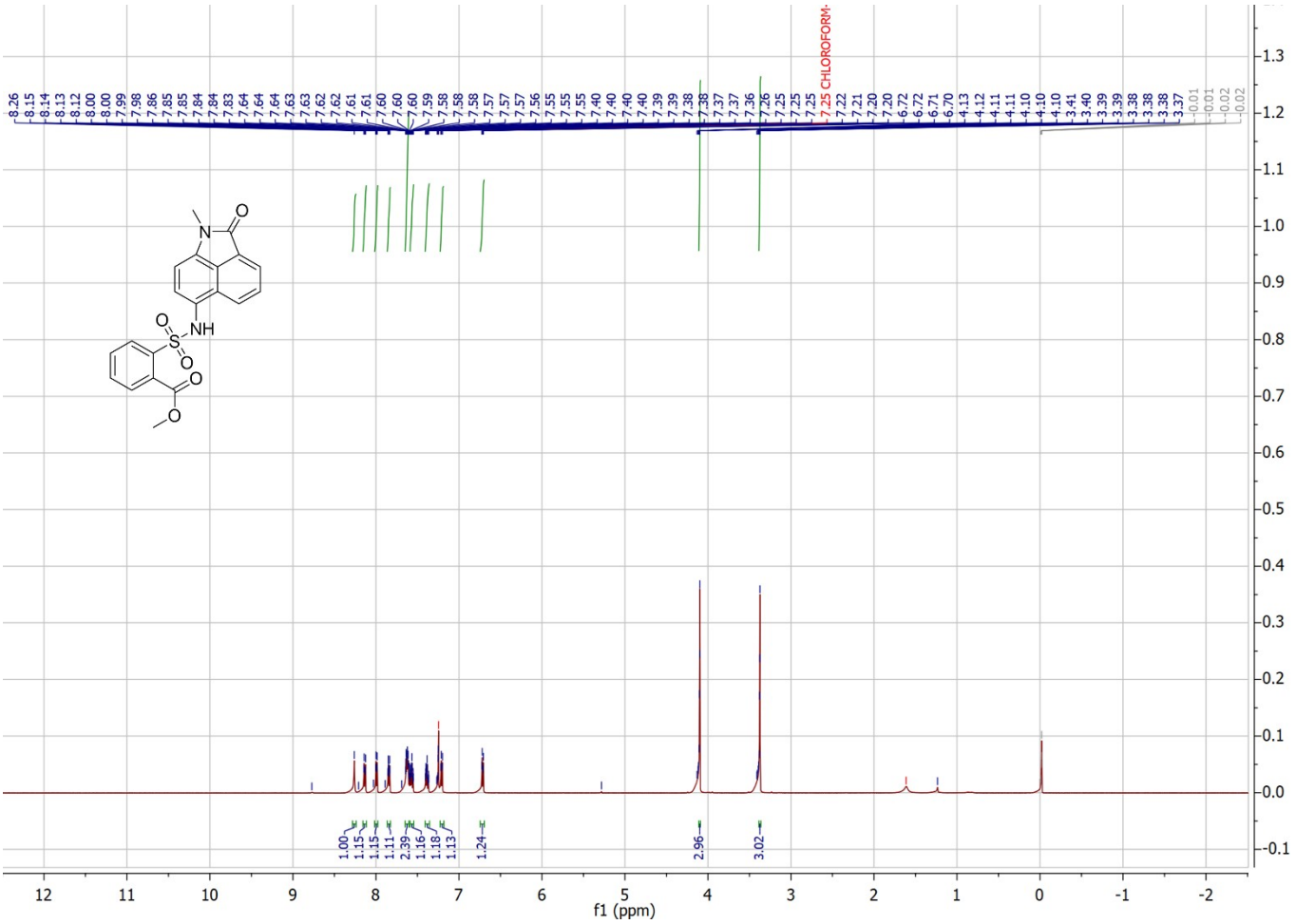

1. Fabian, M. A.; Biggs, W. H., 3rd; Treiber, D. K.; Atteridge, C. E.; Azimioara, M. D.; Benedetti, M. G.; Carter, T. A.; Ciceri, P.; Edeen, P. T.; Floyd, M.; Ford, J. M.; Galvin, M.; Gerlach, J. L.; Grotzfeld, R. M.; Herrgard, S.; Insko, D. E.; Insko, M. A.; Lai, A. G.; Lelias, J. M.; Mehta, S. A.; Milanov, Z. V.; Velasco, A. M.; Wodicka, L. M.; Patel, H. K.; Zarrinkar, P. P.; Lockhart, D. J., A small molecule-kinase interaction map for clinical kinase inhibitors. *Nat. Biotechnol.* **2005,** *23* (3), 329-336.

2. Bai, P.; Lan, Y.; Patnaik, D.; Wang, H.; Liu, Y.; Chen, Z.; Yuan, G.; Afshar, S.; Striar, R.; Zagaroli, J. S.; Tocci, D. R.; Langan, A. G.; Haggarty, S. J.; Wang, C., Design, synthesis, and evaluation of thienodiazepine derivatives as positron emission tomography imaging probes for bromodomain and extra-terminal domain family proteins. *J. Med. Chem.* **2021,** *64* (19), 14745-14756.

3. Bai, P.; Lan, Y.; Wang, H.; Liu, Y.; Striar, R.; Yuan, G.; Afshar, S.; Zagaroli, J. S.; Tocci, D. R.; Langan, A. G. J. B. C., Synthesis and characterization of a positron emission tomography imaging probe selectively targeting the second bromodomain of bromodomain protein BRD4. *Bioconjug. Chem.* **2021,** *32* (8), 1711-1718.